Hindawi Publishing Corporation
Advances in Acoustics and Vibration
Volume 2012, Article ID 473531, 13 pages
doi:10.1155/2012/473531

Research Article

Sound Scattering by a Flexible Plate Embedded on Free Surface

Eldad J. Avital,[1] Theodosios Korakianitis,[2] and Touvia Miloh[3]

[1] *School of Engineering and Materials Science, Queen Mary University of London, London E1 4NS, UK*
[2] *Parks College of Engineering, Aviation and Technology, Saint Louis University, St. Louis, MO 63103, USA*
[3] *Faculty of Engineering, Tel-Aviv University, 69978 Tel Aviv, Israel*

Correspondence should be addressed to Eldad J. Avital, e.avital@qmul.ac.uk

Received 10 April 2012; Revised 9 August 2012; Accepted 10 August 2012

Academic Editor: Rama Bhat

Sound wave scattering by a flexible plate embedded on water surface is considered. Linear acoustics and plate elasticity are assumed. The aim is to assess the effect of the plate's flexibility on sound scattering and the potential in using that flexibility for this purpose. A combined sound-structure solution is used, which is based on a Fourier transform of the sound field and a finite-difference numerical-solution of the plate's dynamics. The solution is implemented for a circular plate subject to a perpendicular incoming monochromatic sound wave. A very good agreement is achieved with a finite-difference solution of the sound field. It is shown that the flexibility of the plate dampens its scattered sound wave regardless of the type of the plate's edge support. A hole in the plate is shown to further scatter the sound wave to form maxima in the near sound field. It is suggested that applying an external oscillatory pressure on the plate can reduce significantly and even eliminate its scattered wave, thus making the plate close to acoustically invisible. A uniformly distributed external pressure is found capable of achieving that aim as long as the plate is free edged or is not highly acoustically noncompact.

1. Introduction

This work looks at sound scattering by a flexible plate embedded on the surface of calm water. The latter is a simplified model for flexible structures embedded on free surface such as manmade platforms which were investigated previously for their interactions with gravity surface waves, for example, [1–3]. Interest resides with the interaction between an incoming sound wave and the structural dynamics of the plate embedded over the free surface and particularly how it affects the near and far sound fields. Examples for the significance of such interaction can be found in marine engineering, for example, ships and offshore structures, as well as in aeronautical, mechanical, and nuclear engineering [4]. Further interest resides in the ability of the flexibility of the thin structure to dampen sound scattering, whether naturally, that is, with no external intervention or by adding some external controlled load acting on the plate.

Sound generated by plate vibrations has been mainly investigated in relation to loud speaker applications. For example, Suzuki and Tichy [5] looked at sound generated by a circular plate supported on its edge by an infinite baffle. Resonance frequency calculations were carried out using the Raleigh integral and Bessel function series expansions. Mellow and Kärkkäien [6] looked at the case of a circular membrane embedded in an infinite baffle. Good agreement was found between a Bessel series solution and a finite element model (FEM) as long as the latter was well resolved. The acoustic pressure field and the impedance of the membrane were calculated. The case of an infinite elastic plate was with dealt by Johansson et al. [7], seeking a governing equation that involves only the acoustic pressure. They found two possible equations, one for the axisymmetric case and another for an antisymmetric case. Smith and Craster [8] developed numerical and asymptotic methods based on the Fourier expansions for sound scattered by elastic plates embedded in rigid baffles. Further solutions for circular and rectangular plates with various kinds of edge support can be found in Junger and Feit [9].

The case of a plate embedded between two immiscible fluids of different phases has been less investigated and, when it was, it has been mostly for incompressible fluids. Kwak and Han [10] used a Fourier-Bessel series expansion to investigate the effect of an incompressible fluid depth on the vibration of

a circular plate resting on a free surface. Good agreement was found with experiments showing that the fluid depth could be neglected if it were larger than the plate's diameter. Zilman and Miloh [1] derived a nondimensional stiffness parameter to show the thresholds for a circular floating plate to behave as a flexible mat or a rigid body under the effect of surface waves. Khabakhpasheva and Korobkin [2] investigated the hydroelastic behaviour of plates modeled as an Euler beam whether floating or attached to the sea bottom by springs. Sturova [3] studied analytically the effect of surface wave pressure on flexible rectangular plates, finding wave guides for elongated plates. Bermúdez et al. [11] considered the case of a rectangular plate placed as a lid over a cavity filled with compressible fluid. FEM was used to calculate the resonance frequencies. A cavity sealed by a flexible rectangular plate was also considered by Leppington and Broadbent [12]. The effects of a plane wave coming from outside of the cavity and a point sound source located within the cavity were analyzed. Jeong and Kim [13] investigated the case of a circular plate separating two compressible fluids inside a cylindrical container. Both FEM and the Bessel series expansions were used to yield good agreement. The compressibility effect on the plate's motion was studied, and it was found that as the plate approached the top or the bottom of the container the resonance frequencies decreased significantly.

Recently interest has grown in investigating the possibility of acoustic invisibility of an object, meaning reducing significantly the scattered sound wave field in order to diminish detection as well as improving structural integrity by reducing the effect of acoustic fatigue on nearby structures. Traditionally, invisibility or cloaking has been associated with electromagnetic waves, but interest has expanded towards acoustics. The analogy between the acoustic equations to Maxwell equations for a two-dimensional geometry can be used to derive a coordinate transformation needed to design an acoustic cloaking coat of an anisotropic mass density. Zhang et al. [14] used a similar approach to design a 2D acoustic cloaking structure based on a network of small cavities connected by narrow channels. Water tank experiments showed a reduction of about 6 dB in the scattered field for ultrasound waves impinging on a small scale cylinder of 1.35 cm radius. Active cloaking by point sources located outside of the cloaked region was also studied and demonstrated numerically for two-dimensional acoustics [15]. This required exact knowledge of the incident wave. Another type of active cloaking was also studied by Avital and Miloh [16] who considered an approach where the flexibility of a cylindrical shell was utilized to search for possible configurations of an external load acting on the shell that would result in the demise of the scattered waves. Exact solutions were derived, while the possibility of a discrete load distribution was also discussed.

A thin plate embedded on calm water surface is considered in this study. Only compressibility effects, that is, acoustic waves will be considered. The plate is taken as embedded on the free surface and thus the problem of gravity waves can be linearly divorced from the acoustic problem for calm water surface, for example, Avital and Miloh [16] and Avital et al. [17]. There are two objectives for this investigation; the first is in studying the sound scattering, and the second is in examining the potential ability of diminishing or at least reducing the scattering using a simple distribution of an external load acting on the plate. Interest resides with the effect of the plate's flexibility, utilizing it to reduce the sound scattering as in the approach of Avital and Miloh [16], while also looking at the effects of the type of the plate's edge support and an impurity in the plate modeled as a hole. This is a mixed boundary problem, and a method of solution for the general case when based on the Fourier transform is discussed in the next section. Special intention is given for the circular plate that is still of an engineering interest [1], while presenting a simplified geometry that includes 3D effects. Results are analyzed for the effects of the incoming sound frequency and the type of the plate's edge support, followed by a summary.

2. Mathematical and Numerical Formulation

Both linear acoustic and linear plate dynamics are considered. The plate is assumed to be thin and of an isotropic and homogenous material. It is taken as embedded on the interface between water and air; both are assumed to be at rest. The air's acoustic impedance is very low as compared to the water's impedance, and thus the air-water interface is taken as a free surface, that is, a zero-pressure surface. A monochromatic incident plane wave is assumed mimicking the case of a sound source far from the plate. The water's depth is taken as infinite as the source of the incident sound wave is assumed to be in the far sound field.

There are various approaches to compute sound waves reflected by rigid and elastic structures. They range from analytical methods based on eigenfunction expansions to numerical ones based on finite difference, finite and boundary element, and source substitution methods [18]. In this study, we will concentrate on a solution based on a Fourier transform for the sound field as coupled with a finite difference solution of the plate's dynamics. A similar approach was already used successfully to investigate sound scattering by vertical cylinders [16] and compute the sound generated by the interaction between water flow and vertical cylinders [17]. A secondary solution based on a finite difference scheme in the time-space domain of the sound field will be employed in this study for verification purposes. Further details on this solution are given in the appendix.

2.1. A General Fourier-Transform Approach. A monochromatic incoming plane sound wave propagating towards the free surface is assumed, and thus the acoustic pressure can be taken as $p(x, y, z, t) = P(x, y, z)e^{i\omega t}$, where i is the square root of -1 and ω is the incoming sound wave's frequency. Here x and y are the rectangular horizontal directions and z is the vertical direction pointing downwards, so $z = 0$ is the plane of the free surface (see Figure 1 for illustration). This leads to the following Helmholtz equation as the governing equation for the sound field:

$$\nabla_h^2 P + \frac{\partial^2 P}{\partial z^2} + k_0^2 P = 0, \tag{1}$$

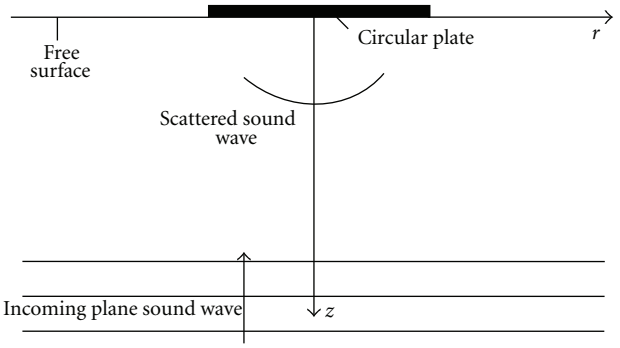

Figure 1: Schematic description of the problem.

where $k_0 \equiv \omega/c$ and c is the water's speed of sound. The operator $\nabla_h^2 P$ is $\partial^2 P/\partial x^2 + \partial^2 P/\partial y^2$ for rectangular coordinates. The boundary condition for P on the free surface is

$$P(x, y, z = 0) = 0, \quad x, y \in \text{outside of the plate}, \tag{2}$$

and on the plate (see [8]),

$$\left.\frac{\partial P}{\partial z}\right|_{z=0} = \rho\omega^2 W(x, y), \quad x, y \in \text{on the plate}, \tag{3}$$

where ρ is the water's density and the plate's deflection w was expressed as $w(x, y, t) = W(x, y)e^{i\omega t}$.

Following Smith and Craster [8], the governing equation for the plate's deflection is taken as

$$D\nabla_h^4 W - \rho_p h\omega^2 W = P + F. \tag{4}$$

The above equation holds for linear structural dynamics, and the reader is referred to Smith and Craster [8] and Gratt [19] for further details on its applicability in structural acoustics and dynamics. The operator $\nabla_h^4 W$ is $(\partial^2/\partial x^2 + \partial^2/\partial y^2)^2 W$ for rectangular coordinates. The plate's bending stiffness D is

$$D = \frac{Eh^3}{12(1-\nu^2)}. \tag{5}$$

E is Young's modulus, h is the plate's thickness, ν is the Poisson's ratio, and ρ_p is the plate's density. The external load f acting on the plate was taken as $f(x, y, t) = F(x, y)e^{i\omega t}$ in (4). There are three possible types of plate edge conditions; clamped, hinged, and free. Clamped condition means no deflection and zero slope of the deflection. Hinged condition means no deflection and no bending moment, and a free edge condition means no bending moment and no shear force. Since the mathematical formulation for these conditions depends on the plate's geometry, that formulation will be given in the implementation section for the circular plate.

The solution of the acoustic pressure P for the Helmholtz equation (1) can be expressed as

$$P = P_{\text{incident}} + P_{\text{scattered}}, \tag{6}$$

where

$$P_{\text{incident}} = e^{i(k_{x0}x + k_{y0}y)} e^{ik_{z0}z}, \tag{7}$$

$$P_{\text{scattered}} = e^{i(k_{x0}x + k_{y0}y)} \iint_{-\infty}^{\infty} A\left(\gamma_x, \gamma_y\right) e^{i\gamma_x x + i\gamma_y y + sz} d\gamma_x d\gamma_y, \tag{8}$$

k_{x0} and k_{y0} are the possible horizontal waves numbers of the incident sound wave indicating an oblique propagation as relative to the free surface. They fulfill the relation:

$$k_{x0}^2 + k_{y0}^2 + k_{z0}^2 = k_0^2. \tag{9}$$

The scattered wave's vertical variation coefficient s is

$$s = \begin{cases} -\sqrt{\widetilde{\gamma}_x^2 + \widetilde{\gamma}_y^2 - k_0^2}, & \widetilde{\gamma}_x^2 + \widetilde{\gamma}_y^2 > k_0^2 \\ -i\sqrt{k_0^2 - \widetilde{\gamma}_x^2 - \widetilde{\gamma}_y^2}, & \widetilde{\gamma}_x^2 + \widetilde{\gamma}_y^2 < k_0^2, \end{cases} \tag{10}$$

where $\widetilde{\gamma}_x \equiv k_{x0} + \gamma_x, \widetilde{\gamma}_y \equiv k_{y0} + \gamma_y$. Expression (10) for the vertical variation coefficient s of the scattered wave fulfills the radiation condition in the vertical direction z, showing that high wavenumbers of γ_x and γ_y are nonradiative, that is, decay exponentially in the z direction, and low wavenumbers are radiative.

The problem comes down to finding the distribution of the Fourier modes $A(\gamma_x, \gamma_y)$ by making the acoustic pressure P fulfill the boundary condition on the plate equation (3) and the boundary condition on the free surface equation (2). There are several approaches of finding this Fourier mode distribution, and a general method will be communicated in a followup study as discussed in the Section 4. The essence of the present study is to assess whether the flexibility of the plate has an effect on the sound scattering and if there is a potential to use that effect to manipulate the scattering to a desired situation. Thus a solution that is rather of a forward simple approach is used in this study. Firstly, a common situation is that the sound emitter of the wave propagating towards the plate-free surface and its associated sound receiver are located at the same place, thus that wave will be emitted as perpendicular to the plate in order to maximize the reflection of the wave towards the sound emitter-receiver. This means that the horizontal incoming wavenumbers k_{x0} and k_{y0} are zero.

Secondly, the form of the scattered wave is of importance, that is, whether it propagates in two dimensions as a cylindrical wave or in three dimensions capable of becoming a spherical wave. Most of the free-surface thin structures are finite in both horizontal directions; thus a three-dimensional propagation has to be allowed in the solution. The simplest form of thin structure to achieve this kind of sound propagation is the circular plate, a form that is still of an engineering interest [1]. This means that the sound field becomes axisymmetric and the Fourier transform in (8) can be replaced by a Bessel-Fourier transform. This is the approach presented in the following.

2.2. The Circular Plate Subject to a Perpendicular Incoming Sound Wave. A finite number of the Bessel-Fourier modes will be computed by requiring the solution to comply with the pressure boundary condition on the plate and free

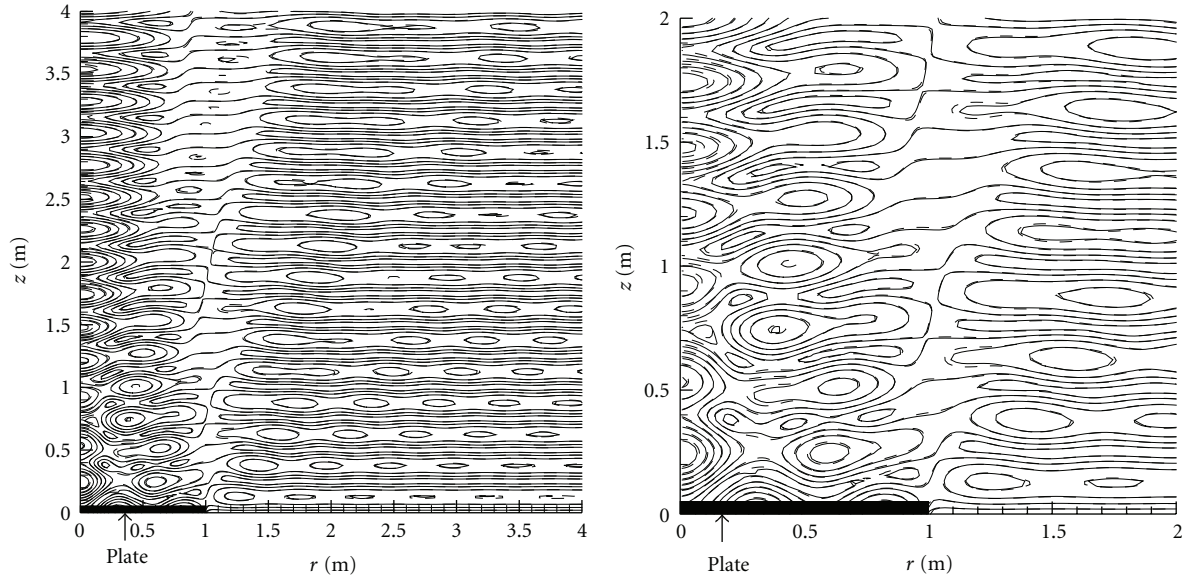

Figure 2: Zoomed views on the contour levels of the pressure amplitude as were calculated by the spectral and time-marching scheme approaches in the presence a rigid floating plate of 1 m radius and an incoming sound wave of 3000 Hz. The computational domain is stretched up to $r = 10$ m and $z = 10$ m. There are nine contour plots ranging from 0.5 to 4.5, where the solid lines denote the spectral solution, and the dashed lines denote the time-marching solution.

surface at a finite number of points. Thus the Bessel-Fourier transform can be written as a series as in (11)

$$P = e^{ik_0 z} + \sum_{m=0}^{M} A_m J_0(\gamma_m r) e^{s_m z}, \tag{11}$$

where r is the radial direction. $\gamma_m(R)$ can be seen as the radial wavenumbers, and they are functions of the computational domain radial length R as explained after (12), where $\gamma_{m=0} = 0$. $J_0(\gamma_m r)$ is the Bessel function of the first kind. The exponential coefficient s_m of the z direction is to fulfill the same conditions as in (10) leading to

$$s_m = \begin{cases} -\sqrt{\gamma_m^2 - k_0^2}, & \gamma_m > k_0 \\ -i\sqrt{k_0^2 - \gamma_m^2}, & \gamma_m < k_0. \end{cases} \tag{12}$$

To ensure series convergence by the Strum-Liouville theory, the radial wavenumbers are determined by taking $dJ_0(\gamma_m r)/dr = 0$ at the radial edge of the computational domain $r = R$ [20]. Taking $R \to \infty$ will make the Bessel-Fourier series in (11) a Bessel-Fourier integral if the mode A_m is rewritten as $\widetilde{A}_m \gamma_m$. However in reality R is taken as finite and it has to be much larger than the plate's radius a to reduce effects of computational domain edge conditions. In a full 3D problem, this will cause a significant computational cost, but for our axisymmetric problem aimed at assessing the validity of using the plate's flexibility on the sound scattering, this computational cost is feasible. It should be also noted that the free surface is a perfect sound wave reflector and it stretches to infinity. Thus one should expect sound wave propagating in the opposite direction of r in order to adjust the pressure over the plate for the existence of an infinite free surface. Solution (11) allows such waves, and again the computational domain radial length R has to be taken of sufficient length in order to account with sufficient accuracy for the effect of the free surface on the pressure field over the plate.

The coefficients A_m are determined by requiring the acoustic pressure P to comply with the boundary conditions at $z = 0$, (2) and (3). Dividing the computational domain side at $z = 0$ to $M+1$ segments then A_m for $m = 0 \cdots M$ can be determined by complying the boundary conditions at the mid points of those segments. At the free surface, this yields

$$\sum_{m=0}^{M} A_m J_0(\gamma_m r_n) + 1 = 0, \quad a < r_n < R, \tag{13}$$

and at the plate's surface,

$$\sum_{m=0}^{M} A_m s_m J_0(\gamma_m r_n) + ik_0 = \rho\omega^2 W_n, \quad r_n < a, \tag{14}$$

where a is the radius of the plate. In case of a central hole in the plate then (13) holds on the free surface inside that hole.

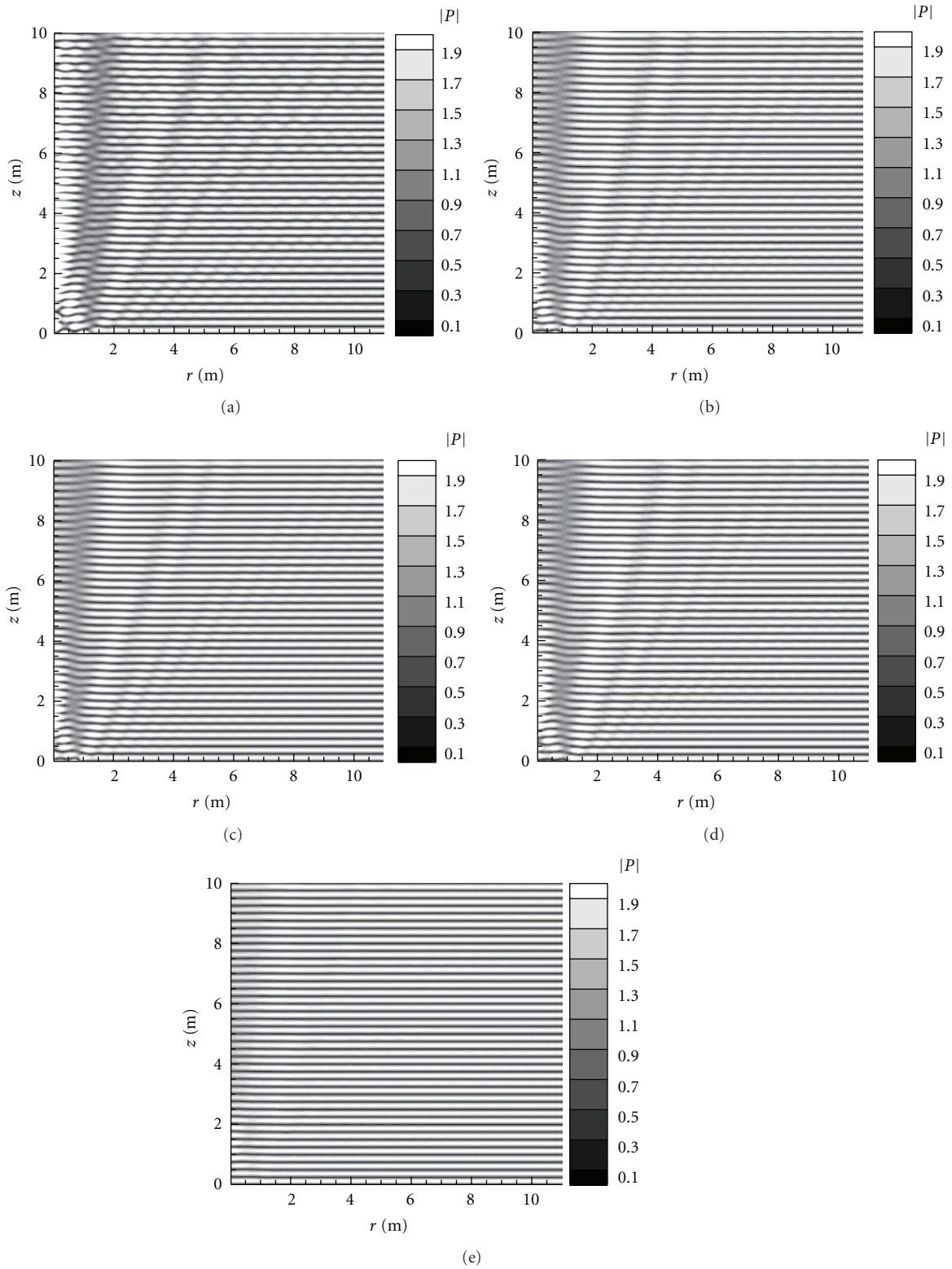

Figure 3: Contour plots of the pressure amplitude as were calculated for (a) rigid plate and aluminium plates of (b) 5 cm thickness and hinged edge, (c) 5 cm thickness and clamped edge, (d) 5 cm thickness and free edge, and (e) 5 mm thickness and hinged edge. The incoming sound wave frequency is 3000 Hz, and the rest of the conditions are as in Figure 2.

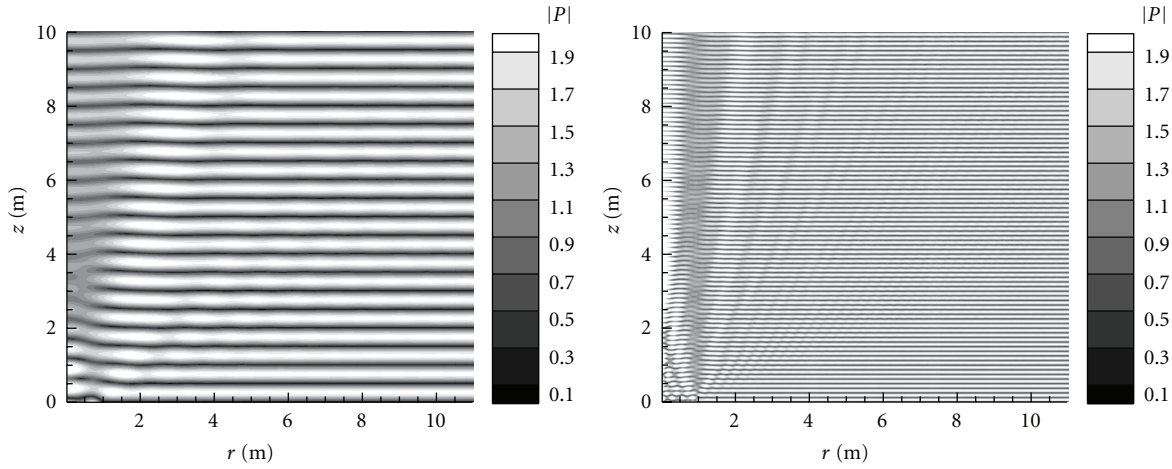

Figure 4: Contour plots of the pressure amplitude as were calculated for a hinged plate of 5 cm thickness and sound frequency of (a) 1500 Hz and (b) 6000 Hz. The rest of the conditions are as in Figure 2.

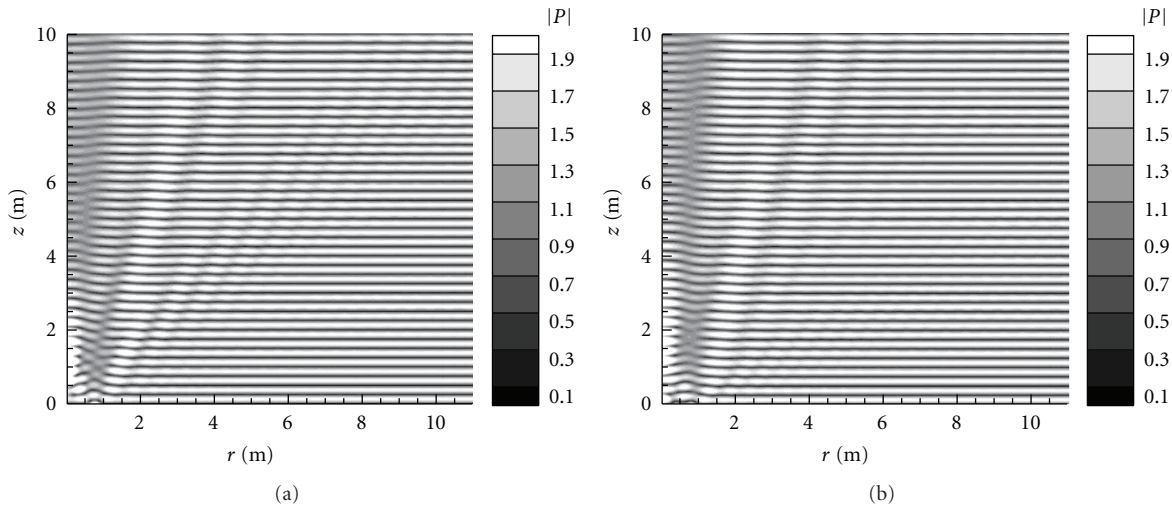

Figure 5: Contour plots of the pressure amplitude as were calculated for sound frequency of 3000 Hz and a hinged plate with a central hole of (a) 0.5 m radius and (b) of 0.25 m radius. The rest of the conditions are as in Figure 4.

The plate deflection W_n at $r = r_n$ is found by solving the deflection equation (4). This solution is subject to three possible edge conditions [21]:

$$\text{Clamped edge:} \quad W = \frac{dW}{dr} = 0$$

$$\text{Hinged edge:} \quad W = \frac{d^2W}{dr^2} + \frac{\nu}{r}\frac{dW}{dr} = 0$$

$$\text{Free edge:} \quad \frac{d^2W}{dr^2} + \frac{\nu}{r}\frac{dW}{dr} = \frac{d^3W}{dr^3} + \frac{1}{r}\frac{d^2W}{dr^2} - \frac{1}{r^2}\frac{dW}{dr} = 0. \tag{15}$$

These are implemented at the outer edge of the plate and at an inner edge if there is a hole in the plate. Symmetry assumption is used for $r = 0$. The solution can be found analytically using a Bessel series or by a finite difference scheme as was used in this study. Thus the solution for W_n can be written as

$$W_n = L_{ns}^{-1}\left[1 + \sum_{m=0}^{M} A_m J_0(\gamma_m r_s) + F_s\right]. \tag{16}$$

The central finite difference schemes used to approximate (4) are five points stencils and are at least of second order. The result is a pentadiagonal matrix for L_{ns} which can be solved rapidly using LU decomposition [22].

Equations (13), (14), and (16) result in a full matrix equation for the coefficients A_m, which can be solved using LU decomposition [22]. This is basically a collocation method. However, numerical experimentation showed that the matrix may become ill conditioned, that is, close to be singular and thus causing difficulties to the matrix solver. Therefore a least square operation was added with respect

to A_m and with a linear weight function of r. This is similar to the operation usually used to determine the coefficients of a Fourier-Bessel series, and it led to a much better conditioned matrix. The resulting equation with respect to the wavenumber k_I, where $I = 0 \cdots M$, is

$$\sum_{n=0}^{Na} r_n \left[s_I J_0(\gamma_I r_n) - \rho\omega^2 \frac{\partial W_n}{\partial A_I} \right] \times \left[\sum_{m=0}^{M} A_m s_m J_0(\gamma_m r_n) + ik_0 - \rho\omega^2 W_n \right] + \sum_{n=Na+1}^{M} r_n J_0(\gamma_I r_n) \left[\sum_{m=0}^{M} A_m J_0(\gamma_m r_n) + 1 \right] = 0, \quad (17)$$

where

$$\frac{\partial W_n}{\partial A_I} = L_{ns}^{-1}[J_0(\gamma_I r_s)]. \quad (18)$$

Na is the number of grid points on the plate, and it was assumed that there is no hole in the plate. If there is a central hole in the plate, then an additional term similar to the second term has to be added to (17) to account for the free surface in that hole. Equation (17) is a full square matrix with $M + 1$ unknowns of A_m and it can be solved using a pivoted LU decomposition [22].

2.3. Forced Plate Deflection and Cloaking. One of the main aims of this study is to cause the sound wave reflection from the plate to mimic a surface of zero impedance, that is, free surface. This means acoustic cloaking and by expression (11) one gets

$$A_0 = -1, \qquad A_m = 0, \quad m = 1 \cdots M. \quad (19)$$

Thus the pressure gradient $\partial P/\partial z$ over the plate becomes $2ik_0$, yielding a uniform deflection W over the plate by (3):

$$W(r) = \frac{2ik_0}{\rho\omega^2}. \quad (20)$$

Such situation is possible only for a free edged plate, leading by (4) to a uniform external pressure F as required for cloaking the plate:

$$F(r) = \frac{-2ik_0\rho_p h}{\rho}. \quad (21)$$

This solution of a uniform load is valid for any geometrical form of the plate and not just circular as long as the plate is free edged.

For clamped or hinged plates, a significant reduction in the scattered sound may be possible if the following target (cost) function Q can be minimized:

$$Q = (1 + A_0)^2 + \sum_{i=1}^{M} A_i^2. \quad (22)$$

Q stands for the acoustic power embedded inside the scattered wave as it differs from the standing wave caused by the free surface. If $Q = 0$, the sound field is as of only as in the presence of the free surface. As the incoming pressure amplitude is taken as one, Q also represents a nondimensionalised scattering cross-section of the plate. Minimization of Q can be achieved by varying F and using the Powell optimization algorithm, which is widely available [22]. However for practicality reasons only the case of a uniform distribution of F is discussed in the next section.

3. Results and Discussion

3.1. Validation. Comparisons between the spectral and the time marching solutions are shown in Figure 2 for a rigid circular plate of a radius of 1 m and sound frequency of 3000 Hz. The latter is in the lower end of low frequency sonar and corresponds to a wave length of 0.5 m, where the speed of sound was taken as of fresh water, that is, 1500 m/s. The incoming sound wave amplitude P was taken as 1 Pa, taking into account that this is a linear problem. The computational domain length was taken as 10 m in the vertical and radial directions with a grid resolution of about 30 points per wave length of the incoming wave. A buffer zone was added to the computational domain of the time marching scheme for $10\,\text{m} < r < 12.5\,\text{m}$ having the same grid resolution as inside the computational domain. The computational domain for the spectral solution extended up to 100 m, damping waves reaching its radial boundary by about 20 dB as compared to the plate's edge. Reducing the radial length of the computational domain from 100 m to 50 m showed very little effect on the spectrum of the various modes and in particular on the radiating modes. Thus the radial length of the computational domain was determined as sufficiently long to account for the free surface effect on the plate's scattered sound and damp any noticeable effect of the radial wavenumbers in (11) being of a finite set as determined by the radial edge condition used for series convergence. The spectral solution grid resolution was about 25 points per wave length of the incoming wave. Doubling that grid resolution showed very little effect on the results. The pressure amplitude contours were computed and compared with the time-marching results.

Very good agreement is revealed between the two solutions as seen in the overall contour plots of the pressure amplitude seen in Figure 2(a) and in the vicinity of the rigid plate in the zoomed view of Figure 2(b). The contour lines corresponding to the two solutions overlap each other as such that they are almost indistinct, showing the very good agreement between the two solutions. Thus the spectral solution has been verified for a rigid plate as in comparison to the time-marching solution. The solution of the plate's deflection equation (4) was verified against known static solutions [23]. Furthermore the analytical solution for the optimised external pressure F required to cloak the free edged plate (21) was also verified against the numerical solution of the spectral solution according to (17).

3.2. Scattered Sound Field and the Plate's Flexibility. The effect of the plate's flexibility can be observed in Figure 3. The grid size, resolution, and sound frequency are similar to those as in Figure 2. The plotted contour levels of the pressure amplitude $|P|$ are of the level expected for sound reflection from the free surface. This was done for purpose of further clarity when considering the grey scale of the contour plots. In fact the sound field reflected by the rigid plate reached a level of $|P|$ of about 4.5 times the incoming wave amplitude around the centre line $r = 0$ as can be seen in Figure 2. Replacing the rigid plate by a flexible one made of aluminium AL2024 T3 and of 5 cm thickness reduced that pressure peak to 3.5 but did not change much the pattern of the sound field as can be seen for the cases of clamped, hinged, and free-edges plates illustrated in Figures 3(b), 3(c), and 3(d), respectively. The wave scattered by the plate concentrates in a narrow beam propagating perpendicular to the plate and widens mildly as it gets further away from the plate. The plate flexibility also reduced the level $|P|$ just over the plate, while changing its edge condition from clamped to hinged and then free-edged extended the region of high pressure over the plate from two lobes to three lobes as seen when comparing Figure 3(b) to Figure 3(d). Finally, reducing the plate's thickness from 5 cm to 5 mm reduces considerably the wave scattered by the plate as seen in Figure 3(e). Similar behaviour was found for the plates with other types of edge support. This is of no surprise since the bending stiffness of the plate was reduced by a factor of 1000 as compared to the plate of 5 cm thickness, causing the thin plate to behave as having low acoustic impedance.

The effect of the sound frequency on the scattered sound field is illustrated in Figure 4 for the aluminium plate of 5 cm thickness and hinged edge. Computational grid resolution as relative to the sound wave length was kept the same as in the previous calculations, and the plotted contour levels were kept the same as well. As in the sound field with the frequency of 3000 Hz, both sound fields of 1500 Hz and 6000 Hz frequencies show most of the wave scattered by the plate to concentrate in a beam above the plate. The widening of that beam as it stretches away from the plate is not affected much by the frequency. The 1500 Hz sound field shows a preservation of the wave fronts with a spatial lag difference between the zone above the plate and that further away from the plate in the radial direction. On the other hand, the 6000 Hz sound field shows a more complicated structure of sound waves with higher pressure levels near the centre of the scattered wave beam with further longitudinal troughs coming from the edge of the plate. This can be attributed to the fact that the plate is a noncompact object, that is, its length scale is much longer than the sound wave length. In this manner, the reflected sound field is similar to that found near noise barriers used to shield noise sources with a wave length much shorter than the height of the noise barrier.

To summarize the cases studied in Figures 3 and 4, values of the pressure load acting on the plate and expressed as the pressure amplitude averaged over the plate's surface are given in Table 1. It is seen that the pressure load is not much affected by the edge condition of the plate, whether the hinged condition of Figure 3(b), clamped of Figure 3(c), and free of Figure 3(d). However, taking the plate as rigid increases noticeably the pressure load while reducing the plate's thickness to 5 mm reduces significantly the pressure load. The latter yielded the reduced wave field scattered by the plate as was seen in Figure 3(e). The incoming wave frequency has a stronger effect on the plate's pressure load than the plate's edge condition as can be seen from Table 1. Increasing the frequency from 1500 Hz (Figure 4(a)) to 3000 Hz (Figure 3(b)) and 6000 Hz (Figure 4(b)) causes a monotonous increase in the pressure load. This is related to the increase in the presence of the wave field scattered by the plate as is seen in the corresponding figures.

The case of an impurity in the plate modelled as a central hole was also tackled and is illustrated in Figure 5 for hinged plates and a sound frequency of 3000 Hz. The computed sound fields resemble those seen for the full plates of Figure 3, that is, a beam of scattered wave above the plate, mildly expanding as it propagates further from the plate. The zone of high pressure level inside the beam is shortened due to the hole in the plate as expected. Instead of two to three lobes of high pressure over the plate, there is only one lobe for the plate with a hole of 0.5 m radius, extending to two lobes if the hole is reduced to a radius of 0.25 m. Interestingly the plates with a central hole also exhibit radiation from their inner edge to form a peak in the scattered wave beam around $r = 0$ as can be seen particularly for the large hole case of 0.5 m radius as seen in Figure 5(a).

To further illustrate the effect of the central hole, values of the pressure load on the plate are given in Table 2 for several radii of the hole, hinged, or clamped conditions and a wave frequency of 3000 Hz. It is seen that for holes that are not too large, that is, 0.6 m or less, the effect of the hole on the pressure load is mild. However, increasing the hole's radius to 0.8 leads to a ring of a width of 0.2 m, which is compact as relative to the incoming wave length of 0.5 m, resulting in a significant change in the pressure load. It significantly decreases for the hinged condition, a trend that was also seen for the full plate case when it was made more compact by reducing the wave frequency, see Table 1. On the other hand the clamped condition stiffens the plate by its zero deflection-slope requirement, causing a higher pressure load.

3.3. Cloaking and Wavenumber Spectra. The derivation in Section 2 showed that uniform external pressure acting on a free-edged plate can alter the sound wave scattered by the plate to mimic completely the wave reflected by the free surface, that is, achieving complete cloaking within the limits of the theory. Therefore it is attractive to examine that approach for plates with other types of edge support. Although clearly it will not be able to achieve complete cloaking, it may still achieve significant reduction in the scattered wave as compared to that reflected by the free surface. Such approach was used to compute the sound fields shown in Figure 6 for the hinged plate and subject to sound frequencies varying of 1500 Hz and 3000 Hz. The target function Q of (22) was minimized by varying the uniform pressure F until a minimum was achieved, where that Q denoted the plate's scattered acoustic power. The

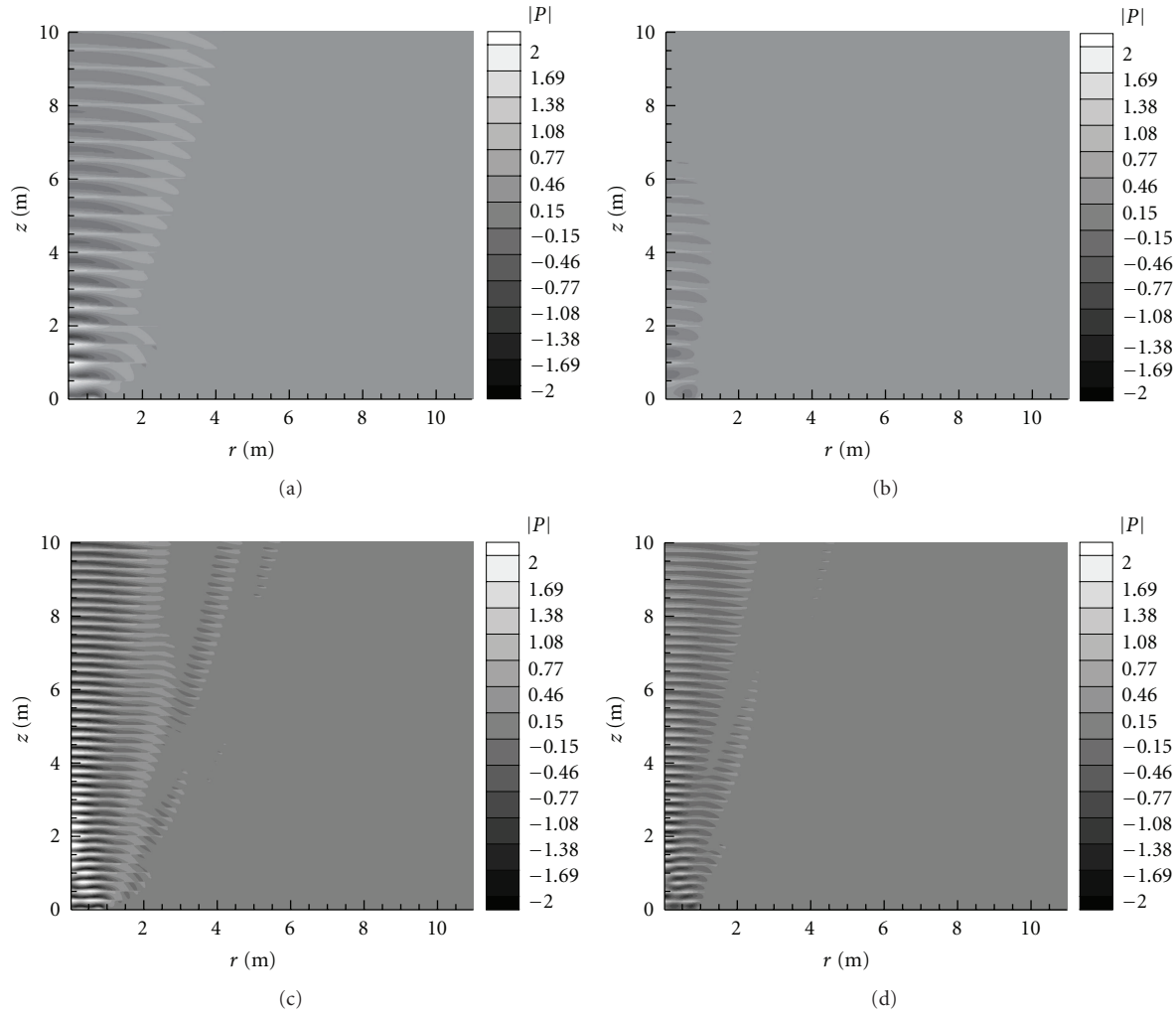

Figure 6: The effect of an optimised external uniform force as it is shown by the pressure amplitude differences between the fields reflected by the plate and free surface, and the free surface only. The sound frequencies and the hinged plate conditions are (a) 1500 Hz with no external force, (b) 1500 Hz with an external uniform force, (c) 3000 Hz with no external force and (d) 3000 Hz with an external force. The rest of the conditions are as in Figure 4.

Table 1: The pressure amplitude averaged over the plate's surface as corresponding to the cases in Figures 3 and 4. The pressure is expressed as relative to the incoming pressure amplitude of 1 (Pa).

Case	Figure 3(a)	Figure 3(b)	Figure 3(c)	Figure 3(d)	Figure 3(e)	Figure 4(a)	Figure 4(b)
Pressure	2.1068	1.6907	1.6845	1.7778	0.3365	1.2457	1.9754

optimised value of F was found to be close to the analytical value derived just for the free-edged plate in (21), but also having a small real part and not just an imaginary part as in (21).

A significant reduction in the plate's acoustic signature was achieved for the low sound frequency of 1500 Hz, as seen by comparing Figures 6(a) and 6(b), where the sound field reflected by just the free surface was subtracted from the overall field for clarity. A less profound reduction in the acoustic signature is seen in Figures 6(c) and 6(d) for the sound frequency of 3000 Hz. This can be understood on the ground that the plate is no longer a compact object as compared to the incoming sound wave length of 0.5 m. Thus a uniform pressure distribution is less likely to be effective in influencing the scattered wave field. Nevertheless a noticeable reduction in the sound field can be observed.

The effect of the sound frequency on the ability to reduce the plate's acoustic signature, that is, achieving acoustic invisibility is shown in Figure 7 for hinged and clamped plates. The ratio of the optimised scattering cross-section is defined as $Q(F_{\text{optimised}})/Q(F = 0)$. This ratio was calculated at various frequencies with intervals of 500 Hz, and a curve of high-order polynomial was plotted to best fit the computed ratios. As already presented in the analysis of Figure 6, this

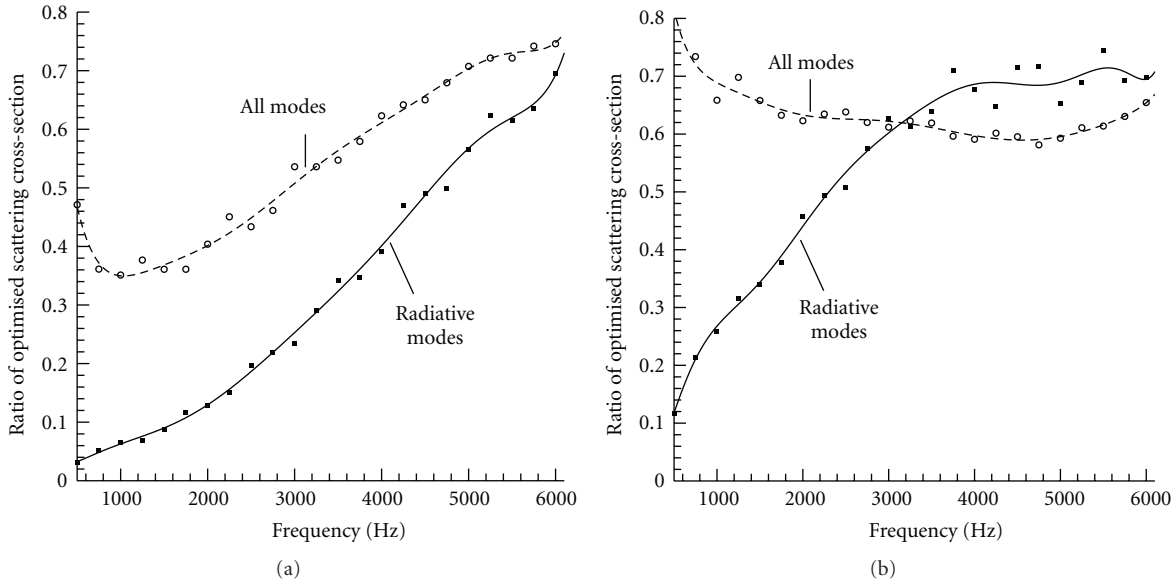

Figure 7: The variation of the optimised scattering cross-section with the sound frequency for (a) hinged and (b) clamped plates, where the cross-section ratio is defined as $Q(F_{\text{optimised}})/Q(F = 0)$. The symbols denote the actual computed values, and the lines are best fitted to those values using polynomials of 8th order. The rest of the conditions are as in Figure 4.

Table 2: The effect of the central hole's radius on the pressure amplitude as averaged over the plate's surface. The pressure is expressed as relative to the incoming pressure amplitude of 1 (Pa), and the rest of the conditions are as in Figure 5.

Central hole's radius (m)	0	0.2	0.4	0.6	0.8
Hinged plate, pressure	1.6907	1.6922	1.5616	1.7017	0.3038
Clamped plate, pressure	1.6845	1.6218	1.6810	1.5069	2.599

kind of active cloaking approach is more effective in the compact range, that is, the lower frequency. Furthermore the reduction in the far field scattering is much more profound than in the near field for both plates in the compact case, which is good news. The hinged plate shows a higher ability to achieve reduced scattering cross-section than the clamped plate. This is because of the higher flexibility of the hinged plate as compared to the clamped plate. The clamped plate losses the ability to reduce significantly the scattered far field sound already at a frequency of 3000 Hz, that is, at an incoming wave length of 0.5 m which is half of the plate's diameter. On the other hand the hinged plate still manages to achieve a reduction of about 6 dB in the scattering cross-section, the same level that was reported for the passive cloaking study of metamaterials by Zhang et al. [14].

To further understand the effect of cloaking, plate's flexibility, and sound frequency, the distributions of the spectral mode amplitudes composing the target function Q were plotted for the sound frequencies of 1500 Hz, 3000 Hz, and 6000 Hz. All mode distributions show a pattern of lobes in Figure 8, which points to a wavenumber leakage or energy transfer between the modes. This happens due to the presence of the plate which, if rigid, introduces a coupling between the modes by forcing the condition of zero-pressure gradient on the plate. Introducing flexibility increases the energy transfer between the modes and pushes more energy towards the nonradiating higher wavenumbers, thus explaining the reduction in the scattered wave field amplitude of the flexible plates seen in Figure 2 as compared to the rigid plate. Changing the edge condition from hinged to clamped or free-edged affected the lobes pattern of the amplitude distribution, pointing again to the effect of the plate's flexibility on energy transfer between the Fourier-Bessel modes. The modes' amplitudes are much reduced for the cloaked cases, particularly for the low frequency of 1500 Hz, affecting mostly the radiating modes as already seen in Figure 7. As the frequency increases, the success in reducing those modes is reduced although some reduction is still achieved even for the frequency of 6000 Hz.

4. Summary

Sound wave scattering was considered as caused by a flexible plate embedded on the surface of calm water. The water surface was taken as free surface and thus modeled as a zero-pressure surface. The aim of the study was to assess the effect on the plate's flexibility on the sound scattering and particularly whether there was a potential in using that flexibility to affect the scattering. An incoming plane monochromatic sound wave was assumed. Linear acoustics and plate's dynamics were used to obtain solutions for

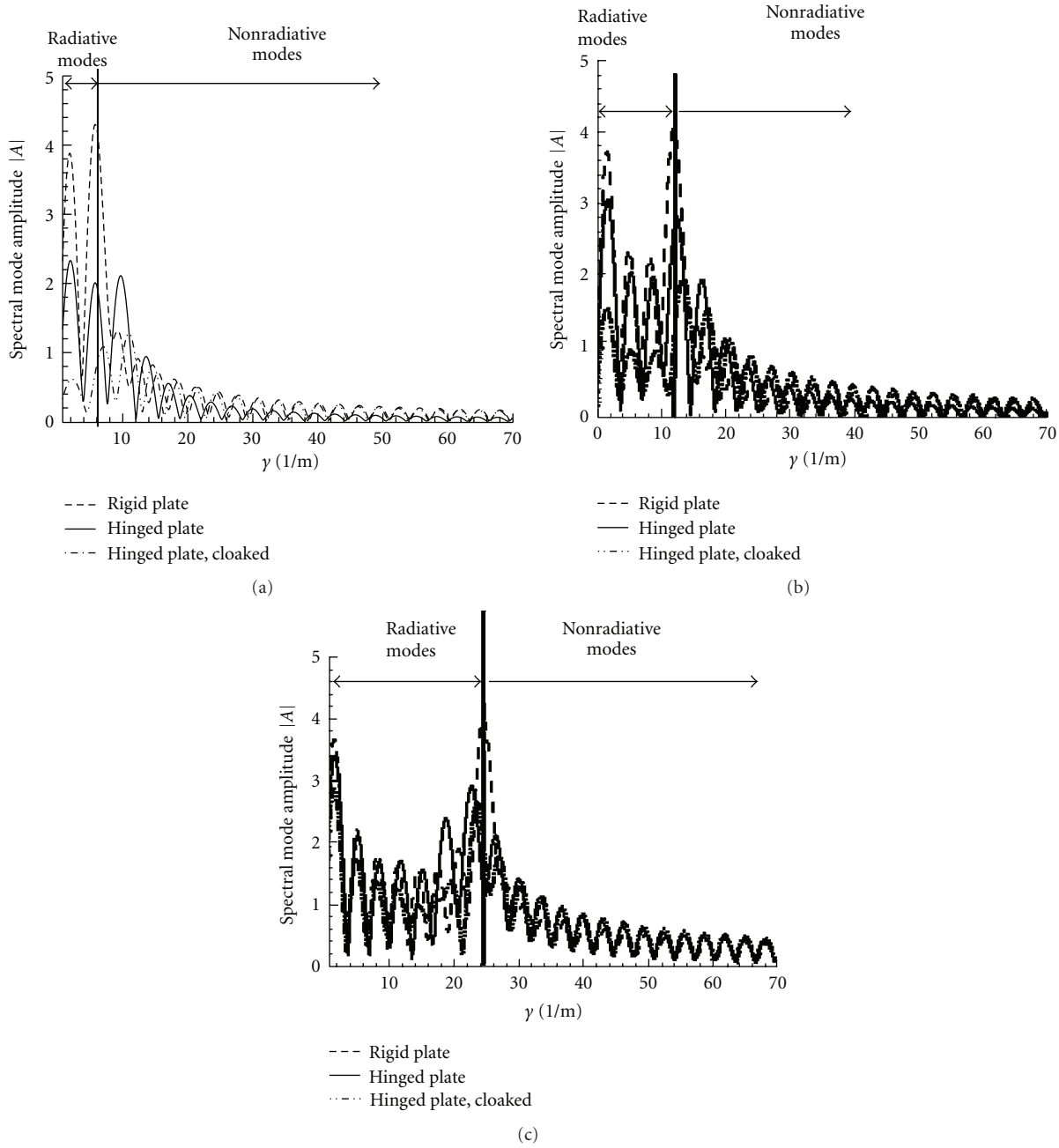

Figure 8: Radial wavenumber spectra of the scattered sound wave for the hinged plate and frequencies of (a) 1500 Hz, (b) 3000 Hz, and (c) 6000 Hz. The mode amplitudes were normalized as relative to the plate's radius. The rest of the conditions are as in Figure 4.

the scattered sound field and plate's deflection. A solution approach based on a Fourier transform of the sound field was introduced. The solution was simplified for the case of a circular plate subject to an incoming perpendicular wave, representing a simplified case of three-dimensional sound propagation. The pressure Fourier modes were coupled to the plate's deflection using central finite-difference schemes.

The combined spectral-finite difference solution was validated against a time-marching simulation of the scattered wave and known solutions of the plate's deflection. It was found that the plate's flexibility reduced the plate's scattered wave by transferring some of its energy from radiating to nonradiating modes. The scattered wave concentrated in a relatively narrow beam propagating perpendicular to the plate. A high-pressure zone was found near the centre of the beam, and such zone decreased but did not vanish when a large hole was introduced at the centre of the plate. This was attributed to sound radiation from the inner edge zone of the plate.

The possibility of reducing the plate's acoustic signature, that is, cloaking was also investigated. This means making the plate acoustically invisible by changing the character of its scattered sound wave to resemble as much as possible that of the sound wave reflected by the free surface. For

this purpose, the approach of applying an external pressure distributed uniformly over the plate and oscillating at the sound frequency was suggested. It was shown theoretically that such approach could achieve complete cloaking for a free-edged plate subject to a perpendicular propagating sound wave and within the limits of the linear theory.

Computations showed that the approach of an external pressure uniformly distributed over the plate could be also effective to achieve good degree of cloaking as long as the plate is not highly noncompact. The radiating modes were particularly reduced as was shown for a hinged plate. It should be noted that the ratios between the plate's length scale (radius) and the incoming sound wave length investigated in this study were of levels similar to those in the study of Zhang et al. [14], where a cloaked cylinder of 13.5 mm radius was subject to incoming sound wave length of 23.5 mm or higher. Thus the proposed method of applying a uniform pressure can present an alternative approach to metamaterials, provided that further work is put on investigating effective implementations. A general method of computing sound scattering for noncircular plates and an oblique incoming wave can be based on finding the influence (Green) functions of discretized segments of the plate. Summing those influences into the pressure condition over the plate will yield a full matrix equation for the pressure values acting on the plate's segments. The contribution of another influence function accounting for the effect of the plate's deflection will have to be added. This approach is of the boundary element methodology, and it will be communicated in a separate study.

Appendix

A time marching scheme was used as a validation tool for the solution of the acoustic pressure obtained by the Fourier-Bessel series solution for a rigid plate. The linear wave equation in the time-space domain can be discretized in time using a central finite-difference scheme of second order as follows:

$$\frac{p_{nm}^{l+1} - 2p_{nm}^{l} + p_{nm}^{l-1}}{\Delta t^2} - c^2 \nabla^2 p_{nm}^{l} = 0, \tag{A.1}$$

where l is the time stage and Δt is the time step of the time marching. A fourth-order central finite difference scheme was used to discretize $\nabla^2 p$ in space. The boundary conditions at $z = 0$, that is, (2) and (3) as written in the time-space domain were discretized using second-order central finite-difference schemes and thus the 4th-order scheme used to discretize $\nabla^2 p$ was replaced by a 2nd-order near the free surface and the plate.

A 1D inlet boundary condition was used for upstream in the z direction:

$$\frac{\partial p}{\partial t} + c\frac{\partial p}{\partial z} = 2\frac{\partial p}{\partial t}\bigg|_{\text{incident}}, \qquad p_{\text{incident}} = e^{i(k_0 z + \omega t)}. \tag{A.2}$$

Boundary condition (A.2) was discretized using a 2nd-order central scheme for the time marching and a one-sided scheme for the spatial derivative. Since at very large radial distances the incoming plane wave propagating in the z direction dominates the sound field, a simple boundary condition of $d^2 p/dr^2 = 0$ was used at the computational domain's radial edge $r = R$. A buffer zone was added in front of the computational domain's radial edge in order to minimize any artificial wave reflections [17, 19]. Scheme (A.1) is an explicit time marching. Thus the CFL limit on Δt was observed in the time marching which started from a zero-pressure condition at $t = 0$ and continued until a steady periodic state was achieved.

Symbols

A_i: Coefficient of the expansion series for the scattered sound wave
a: Circular plate's radius
c: Water's speed of sound
D: Plate's bending stiffness
E: Young's modulus
F: External pressure acting on the plate in the frequency-space domain
f: External pressure acting on the plate in the time-space domain
h: Plate's thickness
J_0: The Bessel function of the first kind and zero order
k_0: Wavenumber of the incoming wave
L_{mn}: Matrix representation of the finite difference discretization of the plate's deflection equation
M: Number of resolved spectral modes
P: Acoustic pressure in the frequency-space domain
p: Acoustic pressure in the time-space domain
Q: Target (cost) function to be minimized in order to cloak the plate
R: Radial length of the computational domain
r: Radial direction
s: Exponential coefficient of the scattered wave in the vertical direction
t: Time
W: Plate's deflection in the frequency-space domain
w: Plate's deflection in the time-space domain
x and y: Rectangular horizontal directions
z: Vertical direction
α: Buffer zone damping coefficient
γ: Wavenumber in the radial direction of the expansion series for the scattered wave
Δt: Time-marching step
ρ: Water's density
ρ_p: Plate's density
ν: Poisson's ratio
ω: Frequency.

References

[1] G. Zilman and T. Miloh, "Hydroelastic buoyant circular plate in shallow water: a closed form solution," *Applied Ocean Research*, vol. 22, no. 4, pp. 191–198, 2000.

[2] T. I. Khabakhpasheva and A. A. Korobkin, "Hydroelastic behaviour of compound floating plate in waves," *Journal of Engineering Mathematics*, vol. 44, no. 1, pp. 21–40, 2002.

[3] I. V. Sturova, "The effect of periodic surface pressure on a rectangular elastic plate floating on shallow water," *Journal of Applied Mathematics and Mechanics*, vol. 70, no. 3, pp. 378–386, 2006.

[4] D. G. Crighton, "The 1988 Rayleigh medal lecture: fluid loading—the interaction between sound and vibration," *Journal of Sound and Vibration*, vol. 133, no. 1, pp. 1–27, 1989.

[5] H. Suzuki and J. Tichy, "Sound radiation from an elastically supported circular plate," *Journal of the Acoustical Society of America*, vol. 65, no. 1, pp. 106–111, 1979.

[6] T. Mellow and L. Kärkkäinen, "On the sound field of a circular membrane in free space and an infinite baffle," *Journal of the Acoustical Society of America*, vol. 120, no. 5, pp. 2460–2477, 2006.

[7] M. Johansson, P. D. Folkow, A. M. Hägglund, and P. Olsson, "Approximate boundary conditions for a fluid-loaded elastic plate," *Journal of the Acoustical Society of America*, vol. 118, no. 6, pp. 3436–3446, 2005.

[8] S. G. L. Smith and R. V. Craster, "Numerical and asymptotic approaches to scattering problems involving finite elastic plates in structural acoustics," *Wave Motion*, vol. 30, no. 1, pp. 17–41, 1999.

[9] M. C. Junger and D. Feit, *Sound, Structures, and Their Interaction*, MIT Press, Cambridge, Mass, USA, 1987.

[10] M. K. Kwak and S. B. Han, "Effect of fluid depth on the hydroelastic vibration of free-edge circular plate," *Journal of Sound and Vibration*, vol. 230, no. 1, pp. 171–185, 2000.

[11] A. Bermúdez, L. Hervella-Nieto, and R. Rodríguez, "Finite element computation of the vibrations of a plate-fluid system with interface damping," *Computer Methods in Applied Mechanics and Engineering*, vol. 190, no. 24-25, pp. 3021–3038, 2001.

[12] F. G. Leppington and E. G. Broadbent, "Acoustic radiation properties of an elastic plate with an infinite baffle and cavity," *Quarterly Journal of Mechanics and Applied Mathematics*, vol. 55, no. 4, pp. 495–510, 2002.

[13] K. H. Jeong and K. J. Kim, "Hydroelastic vibration of a circular plate submerged in a bounded compressible fluid," *Journal of Sound and Vibration*, vol. 283, no. 1-2, pp. 153–172, 2005.

[14] S. Zhang, C. Xia, and N. Fang, "Broadband acoustic cloak for ultrasound waves," *Physical Review Letters*, vol. 106, no. 2, Article ID 024301, 4 pages, 2011.

[15] F. Guevara Vasquez, G. W. Milton, and D. Onofrei, "Exterior cloaking with active sources in two dimensional acoustics," *Wave Motion*, vol. 48, no. 6, pp. 515–524, 2011.

[16] E. J. Avital and T. Miloh, "Sound scattering by free surface piercing and fluid-loaded cylindrical shells," *Philosophical Transactions of the Royal Society A*, vol. 369, no. 1947, pp. 2852–2863, 2011.

[17] E. J. Avital, G. Yu, and J. Williams, "Computation of the flow and near sound fields of a free surface piercing cylinder," *Journal of Computational Acoustics*, vol. 17, no. 4, pp. 365–382, 2009.

[18] Y. J. R. Gounot and R. E. Musafir, "Simulation of scattered fields: some guidelines for the equivalent source method," *Journal of Sound and Vibration*, vol. 330, no. 15, pp. 3698–3709, 2011.

[19] K. F. Gratt, *Wave Motion in Elastic Solids*, Dover, New York, NY, USA, 1991.

[20] F. B. Hilderbrand, *Advanced Calculus for Applications*, Prentice Hall, New York, NY, USA, 1976.

[21] U. S. Gupta, R. Lal, and S. Sharma, "Vibration analysis of non-homogeneous circular plate of nonlinear thickness variation by differential quadrature method," *Journal of Sound and Vibration*, vol. 298, no. 4-5, pp. 892–906, 2006.

[22] W. H. Press, S. A. Teukolsky, W. T. Vettering, and B. P. Flannery, *Numerical Recipes in Fortran*, Cambridge University Press, New York, NY, USA, 1996.

[23] S. P. Timoshenko and S. Woinowsky-Kriger, *Theory of Plates and Shells*, McGraw-Hill, New York, NY, USA, 1959.